

Evaluation of Suburban measurements by eigenvalue statistics

Helmut Hofstetter¹⁾, Ingo Viering²⁾, Wolfgang Utschick³⁾

¹⁾Forschungszentrum Telekommunikation Wien, Donau-City-Straße 1, 1220 Vienna, Austria.

²⁾Siemens AG, Lise-Meitner-Straße 13, 89081 Ulm, Germany.

³⁾Institute for Circuit Theory and Signal Processing, Munich University of Technology, Arcisstraße 21, 80290 Munich, Germany.

hofstetter@ftw.at

Abstract

A MIMO channel measurement campaign with a moving mobile has been conducted in Vienna. The measured data will be used to investigate covariance matrices with respect to their dependence on time. This document focuses on the evaluation of a measurement run in a suburban environment including a walk through a tunnel. The F -eigen ratio is defined expressing the degradation due to out-dated covariance matrices. In addition a SAGE algorithm is used to proof our results. Illustrating the derived methods, first results based on the measured data are shown for a suburban scenarios.

INTRODUCTION

All mobile communication systems incorporating multiple antennas on one or on both sides of the transmission link strongly depend on the spatial structure of the mobile channel. Therefore, a lot of attention has to be paid to explore and to understand the spatial properties of the mobile channel.

Almost all multiple antenna algorithms, including beamforming, diversity as well as MIMO (multiple-input multiple-output) techniques are either directly or indirectly based on spatial covariance matrices and on their properties. A very important point is the stability over time. The longer the covariance matrices are constant, the longer the averaging interval can be chosen and the more reliable are the estimates derived from a covariance measurement.

In order to obtain deeper insights, we will evaluate measurement data with respect to covariance matrices. A wideband MIMO channel sounder was used for the measurement campaign, which was carried out in Vienna last autumn with a moving mobile station.

This paper is focused on the description of the campaign and the derivation of the mechanisms for investigating the covariance matrices. Results from a suburban environment are chosen to illustrate the described methods. Our test scenario includes LOS parts as well as a walk through a tunnel. Main focus is drawn on the propagation effects in and around this tunnel. Regarding the variety of propagation effects of such a measurement run it may become a test scenario for multiple antenna algorithms.

Section I and II describe the equipment and the environment of the campaign. Section III derives the evaluation methods. We show how to extract the covariances from the data, we define a measure for the discrepancy of covariances called the F -eigen-ratio and we will review our implementation of the SAGE algorithm for the DoA estimation. These methods are applied to a scenario of the measurement data in section IV and V. Finally, section VI draws some conclusions.

I. MEASUREMENT SETUP

The measurements were performed by the MIMO capable wideband vector channel sounder RUSK-ATM, manufactured by MEDAV [1]. The sounder was specifically adapted to operate at a center frequency of 2GHz with an output power of 2 Watt. The transmitted signal is generated in frequency domain to ensure a pre-defined spectrum over 120 MHz bandwidth, and approximately a constant envelope over time. In the receiver the input signal is correlated with the transmitted pulse-shape in the frequency domain resulting in the specific transfer functions. Back-to-back calibration before each measurement ensured an unbiased estimate. Also, transmitter and receiver had to be synchronised via Rubidium clocks at either end for accurate frequency synchronism and a defined time-reference.

For studies on MIMO systems, the double-directional nature of the channel must be exploited. Therefore



Fig. 1. Measurement setup at transmitter.



Fig. 2. Measurement setup at receiver in Weikendorf.

two simultaneously multiplexed antenna arrays have been used at transmitter and receiver.

At the mobile station, it is devised to cover the whole azimuthal range. To this end, a uniform circular array was developed by Fa. Krenn [2]. It is made of 15 monopoles mounted on a ground plane and was placed on top of a small trolley (Figure 1). The elements were spaced at 0.43λ (6.45cm) resulting in a diameter of around 30cm in the middle of the 90cm ground-plane. Attention was paid on a height of the transmit antenna of about 1.5m above ground which fits the typical height of pedestrians using their phones. This also matches the COST259 [3] recommendations for mobile terminals.

The receiver was connected to a uniform linear array from T-NOVA, Germany. The antenna is made of eight patch elements spaced at a distance of $\lambda/2$ (7.5cm).

With above arrangement, consecutive sets of 15×8 transfer functions, cross-multiplexed in time, were measured every 21.5ms. Due to the nature of the channel sounder the acquisition period of one snapshot was limited to $3.2\mu\text{s}$ which corresponds to a maximum path length of about 1km.

II. MEASUREMENT ENVIRONMENT

The measurement data used for this paper was conducted during a measurement campaign in Vienna last autumn. For our evaluations we took a typical suburban area in a small town north of Vienna called Weikendorf.

For the Weikendorf measurements the receiver was mounted on a lift in about 20m height (Figure 2) to fit a typical macro cellular environment. All streets within the coverage area of our equipment were measured. Therefore the trolley was moved at speeds of about 5km/h on the sidewalks. This results in a snapshot resolution of more than 8 snapshots per wavelength λ , or per doppler cycle, respectively. The measurement data contains a lot of LOS cases and diffraction over rooftops.

For this work we have chosen a measurement run where the transmitter moves through a pedestrian tunnel. The run is more or less a LOS scenario with diffraction over rooftops. However, changes of the propagation parameters may occur in the tunnel. A map of the measurement run can be found in Figure 3. The Rx-position is marked with a red dot whereas the blue arrow gives the movement of the transmitter.

III. EVALUATION TECHNIQUES

Most beamforming algorithms are based on the spatial covariance matrices [5] [6] $\mathbf{R} \in \mathbb{C}^{K_a \times K_a}$, which contain information about the correlations of the K_a antenna signals. Let $\vec{x}(t)$ be the $K_a \times 1$ antenna data vector. The data covariance matrix is defined as

$$\mathbf{R} = \mathbf{E} \left\{ \vec{h}(t) \cdot \vec{h}(t)^H \right\}. \quad (1)$$

In rich scattering environments and with large element spacings, its structure approaches the identity, whereas in highly correlated scenarios, e.g. with a present line-of-sight, it is getting more and more singular. Hence, it represents the spatial properties of the scenario from the signal processing point of view.

For the wide sense stationarity (WSS) assumption, second order statistics such as the covariance are constant within a certain time interval. However, a varying environment changes the covariance.

In addition, the covariance depends on the carrier frequency, since the visible array topology relates to the wavelength.

In this section, we derive, how we will investigate the time dependency in section IV by help of the sounding measurements.

A. Extraction of Covariances

As already mentioned, the data is available as transfer functions. In the sequel, we will consider the covariance matrices at the base station. First, we extract a 5MHz band of the total band width of 120MHz around the center frequency f_c and transform the transfer functions to the time domain. The 5MHz is a typical bandwidth for third generation systems, e.g. UTRA FDD and UTRA TDD [4]. Starting at a certain time t_0 we set up the covariance matrix by averaging over all values of all impulse responses within a time interval Δt_{avg} , which should not be too long in order to ensure that WSS holds. Since we consider the covariance matrix at the base station, we can use the different mobile antennas to increase the number of available snapshots to achieve a better estimate.

We eliminate the noise contributions by subtracting a noise covariance matrix which is derived from a separate noise measurement.

Finally, the matrices are corrected by a measured calibration matrix \mathbf{C} in order to compensate for linear distortions due to varying properties of the feeder cables, pin diode switches, etc.

The result is a covariance matrix estimate $\mathbf{R}(t_0, f_c)$ which represents the spatial signature of the complete impulse response, i.e. of all channel taps, and which is valid for a certain time t_0 and for a certain carrier frequency f_c . The covariance matrix is calculated from the channel sounder observations by

$$\mathbf{R}(t_0, f_c) = \frac{1}{T_x \cdot \Delta_S} \cdot \mathbf{C}^H \cdot \left[\sum_{k=1}^{T_x} \sum_{s=S_0}^{S_0+\Delta_S} \sum_{\tau=1}^{N_\tau} \vec{h}_k(s, \tau) \cdot \vec{h}_k(s, \tau)^H - \mathbf{R}_{nn} \right] \cdot \mathbf{C} \quad (2)$$

where T_x and N_τ is the number of Tx antennas and the number of delay values, $S_0, S_0+1, \dots, S_0+\Delta_S$ are the snapshot numbers in the time interval $[t_0; t_0+\Delta t_{avg}]$ and \mathbf{R}_{nn} is the estimated noise covariance matrix. The elements of $\vec{h}_k(s, \tau)$ are the τ th impulse response values from transmit antenna k to all

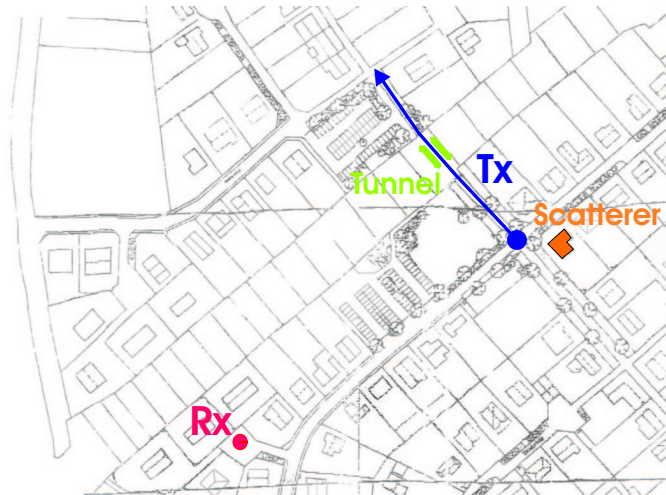


Fig. 3. Map of the measurement route in Weikendorf

receive antennas of snapshot s , which is the inverse fourier transform of the corresponding transfer function in the 5MHz frequency band around f_c .

B. Measure for Covariance Distance

In order to compare the extracted covariance matrices, we will now define a measure expressing the discrepancy between two covariance matrices. Since we consider the eigen structure of the covariances, this measure will be denoted the *F-eigen-ratio*.

We assume, that the actual environment is described by the unknown covariance matrix \mathbf{R} . Instead of the correct matrix, we have knowledge about another covariance $\hat{\mathbf{R}}$ measured in a different scenario, e.g. at another time instance. If we process $\hat{\mathbf{R}}$ and apply the result in the environment \mathbf{R} , we will get a degradation.

Many beamforming techniques are based on the eigenvectors of the signal covariance matrix [5]. Other methods can be viewed as approximations of the eigen methods [6]. Therefore we introduce the eigenvalue decompositions

$$\hat{\mathbf{R}} = \hat{\mathbf{W}} \cdot \hat{\mathbf{\Lambda}} \cdot \hat{\mathbf{W}}^H \quad ; \quad \mathbf{R} = \mathbf{W} \cdot \mathbf{\Lambda} \cdot \mathbf{W}^H \quad (3)$$

where $\hat{\mathbf{W}}$ and \mathbf{W} contain all eigenvectors, and $\hat{\mathbf{\Lambda}}$ and $\mathbf{\Lambda}$ are diagonal matrices with their entries being the corresponding eigenvalues of $\hat{\mathbf{R}}$ and \mathbf{R} . Without the loss of generality, we assume unitary matrices $\hat{\mathbf{W}}$ and \mathbf{W} .

We define the reduced versions $\hat{\mathbf{W}}_F, \mathbf{W}_F \in \mathbb{C}^{K_a \times F}$ of the matrices $\hat{\mathbf{W}}, \mathbf{W}$ to contain the eigenvectors corresponding to the F largest eigenvalues of the covariance matrices $\hat{\mathbf{R}}$ and \mathbf{R} , respectively.

\mathbf{W}_F is used for a low-rank approximation of \mathbf{R} . Hence,

$$\mathbf{\Lambda}_F = \mathbf{W}_F^H \cdot \mathbf{R} \cdot \mathbf{W}_F \quad (4)$$

is a diagonal with the F largest eigenvalues as entries. If we use $\hat{\mathbf{W}}_F$ instead of \mathbf{W}_F for the low-rank approximation of \mathbf{R} , we get

$$\mathbf{R}_{\hat{\mathbf{W}}_F} = \hat{\mathbf{W}}_F^H \cdot \mathbf{R} \cdot \hat{\mathbf{W}}_F \quad (5)$$

which in general is not a diagonal. The traces of the matrices $\mathbf{\Lambda}_F$ and $\mathbf{R}_{\hat{\mathbf{W}}_F}$ are a measure for the collected power applying the low-rank transforms \mathbf{W} and $\hat{\mathbf{W}}$. Hence, the quotient of the traces gives us some knowledge about the power loss in the case of having $\hat{\mathbf{R}}$ available only. The F-eigen-ratio is defined as

$$q_{eigen}^{(F)} = \frac{\text{tr} \{ \mathbf{R}_{\hat{\mathbf{W}}_F} \}}{\text{tr} \{ \mathbf{\Lambda}_F \}} = \frac{\sum_{k=1}^{K_a} \sum_{f=1}^F \lambda_k \cdot |\vec{w}_k^H \cdot \hat{\vec{w}}_f|^2}{\sum_{f=1}^F \lambda_k} \quad (6)$$

with the properties $0 \leq q_{eigen}^{(F)} \leq 1$ and $q_{eigen}^{(K_a)} = 1$. The second form is the element notation, where $\vec{w}_k, \hat{\vec{w}}_f$ and λ_k are the columns and diagonals of $\mathbf{W}_F, \hat{\mathbf{W}}_F$ and $\mathbf{\Lambda}_F$, respectively. The term $|\vec{w}_k^H \cdot \hat{\vec{w}}_f|^2$ accounts for the mismatch of both eigenbases.

The choice of the parameter F depends on the considered algorithm. In many downlink beamforming [7] schemes, $F = 1$ is the only setting of interest, since often a single beam is formed. More beams are not resolvable with a single receive antenna and therefore would interfere with each other. However, considering uplink scenarios or MIMO techniques, larger values might give more insights.

C. The SAGE algorithm

In section IV we will compare the consequences of the covariance matrices with direct estimation of signal directions. We will apply the SAGE (Space Alternating Generalized Expectation Maximization) algorithm in order to jointly estimate the doppler frequency, the delay, the direction of arrival and the doppler frequency for a given number of waves.

The technique is based on *Expectation Maximization* (EM) introduced in [8]. It was shown, that the

maximum likelihood (ML) solution is achieved. In [9] EM was extended to SAGE as an ML parameter estimator for superimposed signals. The resulting implementation is an iterative method similar to interference cancellation. Signal components are reconstructed with already estimated parameters and cancelled from the total signal. This reduces the dimension of the ML problem maintaining the ML performance.

This document follows the proposal of [10], which gives a detailed description how to estimate the mentioned parameters for a number of waves given the received signal.

As we have the impulse responses available instead of the received signal, a slight adaptation was necessary. Concatenating the impulse responses inserting a guard period in between, we interpret the resulting construction as the received signal, where the transmitted pulse shape is assumed to be the response of the receive filter. In our case, the receive filter is a low pass with a width of 120MHz. We approximate this as a rectangle yielding a *sinc*-pulse shape.

Since the SAGE algorithm is not very sensible to the given model order (number of waves to estimate), it was fixed to 15¹. The size of the observation window was 43 snapshots $\hat{=}$ 925ms in total, where we used 3 sequences of 9 consecutive snapshots equally spaced within this window. The first Tx antenna was used only, as the direction of departure was not taken into account. The initialization procedure was similar to [10].

IV. RESULTS

In the previous section, we described the mechanisms for evaluating measurement data. Now, we will show some results where we applied these techniques to the sounding measurements.

Impulse responses of the measurement scenario at $t = 0$ and with the trolley in the tunnel are shown in Figure 4 and Figure 5 respectively. The attenuation in the tunnel is about 25dB higher than in the LOS case.

Figure 6 shows the estimated DoAs for the Weikendorf run at different time stamps. In the beginning there exists a strong LOS component surrounded by weaker scattering paths from trees and buildings. During the first 20 seconds the trolley moves on and the LOS is still valid but, of course, tracks the mobil position (Figure 6a and b). When the trolley approaches the tunnel, the LOS gets diffracted at the entrance and a second path appears (Figure 6c till e). This path has a longer delay and a different DoA from a direction quite similar to that of our starting position. The path comes from the building which is marked in the map 3 as a scatterer. Its power is about 20dB weaker than the former LOS. The walk through the tunnel lasts for about 3 seconds. During this time the path gets the strongest component. On the first meters through the tunnel additional scattering paths round the entrance are visible (Figure 6b) while later on some components near the exit appear (Figure 6e). This components result from trees and bushes which surround the tunnel. After leaving the tunnel the LOS occurs again but of course now from a different direction (Figure 6f).

In addition to our geometric results we have also investigated into the eigenvalue statistics of this mea-

¹A larger choice did not lead to a larger number of waves with significant power

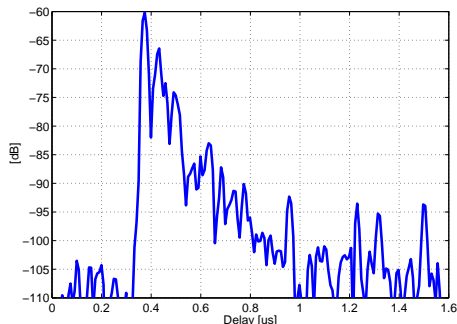


Fig. 4. Impulse response at $t = 0$.

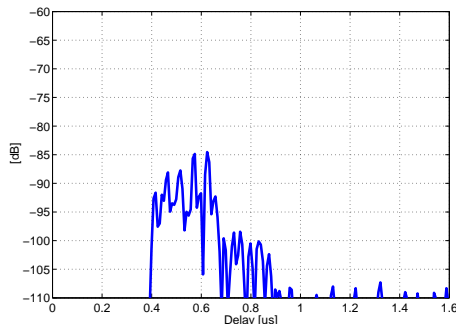


Fig. 5. Impulse response with trolley in the tunnel.

surement run. Therefore the F-eigen ratio, as described above, was used. The covariance matrixes are computed according to 2. They are averaged over in a window of $\delta_s = 50$ snapshots, which is equivalent to $\delta t_{avg} = 1sec$. The covered distance during that interval is in the range of about $5\lambda = 0.75m$.

In addition to the F-eigen ratio for one and two eigenvalues also the beams formed at $t = 0$ are plotted as dashed lines (Figure 8). For this strong LOS-case the F-eigen-ratio for one eigenvalue fits quite well with the beams at $t = 0$ till the trolley disappears in the tunnel. This implies that during the first seconds the F-eigen ratio just describes the run out of the LOS beam at $t = 0$. In the tunnel our second path, as described above, appears from nearly the same direction as the path used as reference for the F-eigen ratio. Since the strongest eigenvalue is always normalized to one, the slow fading does not influence the F-eigen ratio. This results in a strong increase of the F-eigen ratio for the time the trolley is in the tunnel. In addition to the results for the F-eigen ratio at $t = 0$ we have plotted the F-eigen ratio starting at $t = 20sec$ (Figure 9). In this case, the F-eigen ratio decreases in the tunnel because the scattered path at the house is no longer valid as a reference value.

V. INTERPRETATION

Two substantial interpretations can be drawn from the above analysis of the Weikendorf scenario. First, channel state information (CSI) by eigenvalue statistics only seems to be limited in some case. This becomes obvious when spatial properties as DOAs or the corresponding spatial eigenmodes come into the picture. Therefore we simultaneously examine Figures 6 and 7: before and after the tunnel transit the statistics in Figure 7 exhibits one dominant eigenvalue, whereas Figures 6a and 6f illustrate two different corresponding beams. Interestingly, during the tunnel transit the dominant eigenvalues rapidly "change" between the set of the distinguished beams; this demonstrates the importance of the two-rank approximation of the channel. The F-eigen ratio analysis strongly confirms this interpretation both by the above discussed phenomena during the tunnel transit (Figure 8) and by the stability of the eigen ratio for $F = 2$ over almost the complete time range of the measurement (Figure 8 and 9).

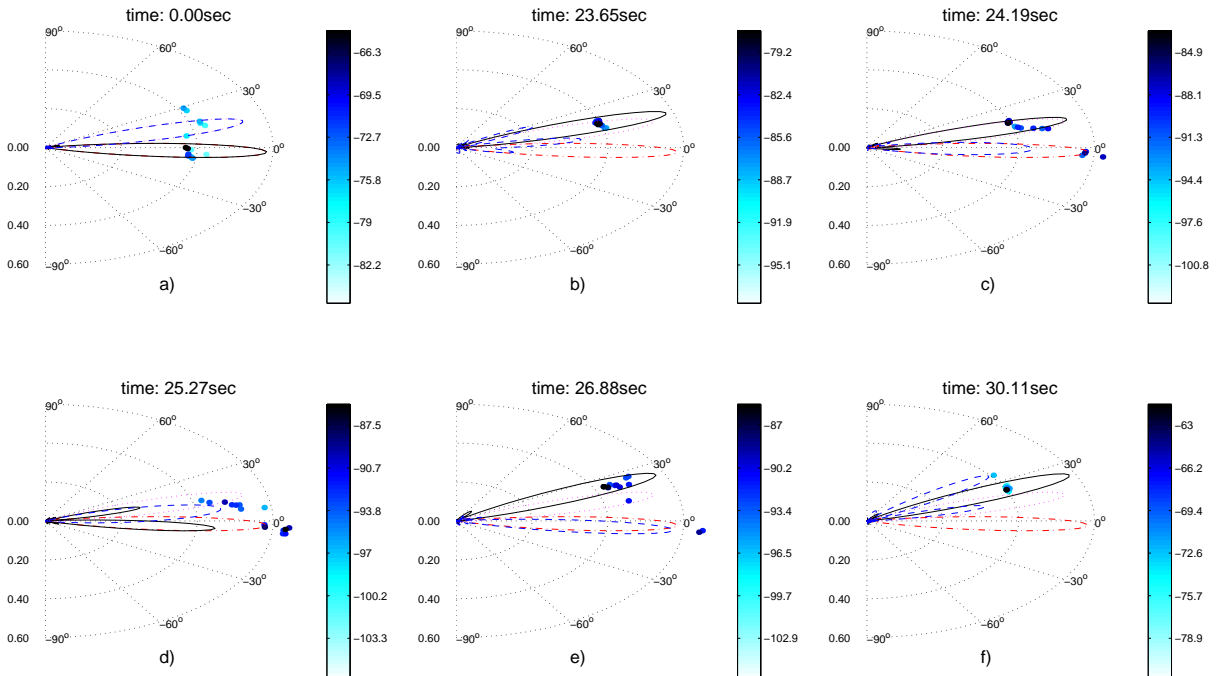


Fig. 6. Estimated DoAs and computed beam patterns for six different time stamps of the Weikendorf measurement

VI. CONCLUSIONS

We presented initial evaluations of a wideband MIMO measurement campaign carried out near Vienna. The focus of this document was on the description of the measurement setup and of proposed evaluation methods which will be used to analyze the measured data in future work.

We defined the F-eigen-ratio which is a measure for the discrepancy of two covariance matrices. The performance of this measure was illustrated by investigating the time dependence of the measured covariance matrices and comparison of this results to our geometrical investigations. A suburban line-of-sight scenario, including a tunnel was chosen.

ACKNOWLEDGMENTS

The authors would like to thank Ingo Gaspard, T-Nova GmbH, for providing the linear receive array and Ralf Müller (*ftw.*) and Christoph Mecklenbräuer (*ftw.*) for continuous support.

REFERENCES

- [1] R. Thomä, D. Hampicke, A. Richter, G. Sommerkorn, A. Schneider, U. Trautwein, W. Wirtzner, "Identification of Time-Variant Directional Mobile Radio Channels," *IEEE Trans. on Instrumentation and Measurement*, vol. 49, no. 2, pp. 357-364, April 2000.
- [2] Walter Krenn, Hochfrequenztechnik GmbH. Am Kanal 27, 1112 Vienna, Austria.
- [3] L. M. Correia (Editor), *WIRELESS FLEXIBLE PERSONALIZED COMMUNICATIONS*, final report of COST Action 259, European Union, 2000.

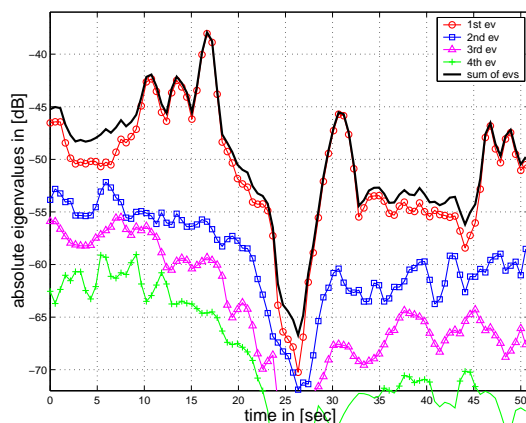


Fig. 7. Eigenvalue statistics over time for the four strongest eigenvalues

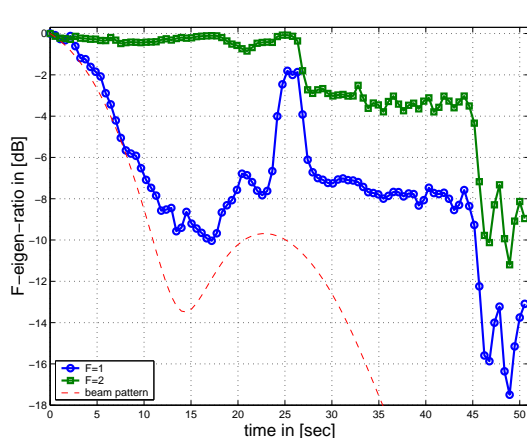


Fig. 8. F-eigen-ratio for Weikendorf measurement over time (Reference covariance matrix at $t = 0$.)

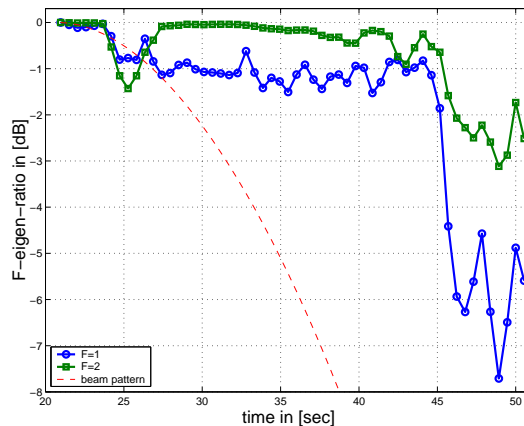


Fig. 9. F-eigen-ratio for Weikendorf measurement over time (Reference covariance matrix at $t = 20$ sec.)

- [4] Specification Home Page, *3rd Generation Partnership Project*, www.3gpp.org/specs/specs.htm
- [5] C. Brunner, W. Utschick, J.A. Nossek, "Exploiting the short-term and long-term channel properties in space and time: eigenbeamforming concepts for the BS in WCDMA," *European Transactions on Telecommunications, Special Issue on Smart Antennas*, VOL. 5, 2001
- [6] I. Vierung, T. Frey, G. Schnabl, "Hybrid Beamforming: Eigen Beamforming on Beam Signals," *International Zurich Seminar on Broadband Communications*, Zurich, Swiss, February 2002
- [7] C. Brunner, J. Hammerschmidt, J.A. Nossek, A. Seeger, "Space-Time Eigenrake and Downlink Eigenbeamformer," *IEEE Globecom 00*, November 2000, San Francisco, USA
- [8] A. P. Dempster, N.M. Laird, D. B. Rubin, "Maximum likelihood from incomplete data via the EM algorithm," *Journal of Royal Statistical Society*, Vol. 39, No. 1, pp. 1-38, 1977
- [9] J. A. Fessler, A. O. Hero, "Space-alternating generalized expectation maximization algorithm," *IEEE Transactions on Signal Processing*, Vol. 42, pp.2664-2677, Oct. 1994
- [10] B.H. Fleury, M. Tschudin, R. Heddergott, D. Dahlhaus, K. I. Pedersen, "Channel Parameter Estimation in Mobile Radio Environments Using the SAGE Algorithm," *IEEE Journal on Selected Areas in Communications*, Vol. 17, No. 3, March 1999